CD94 surface density identifies a functional intermediary between the CD56^{bright} and CD56^{dim} human NK-cell subsets

Jianhua Yu,[1,2] Hsiaoyin C. Mao,[1] Min Wei,[1] Tiffany Hughes,[1] Jianying Zhang,[3] Il-kyoo Park,[1] Shujun Liu,[1,2] Susan McClory,[1] Guido Marcucci,[1,2,4] Rossana Trotta,[1,2] and Michael A. Caligiuri[1,2,4]

[1]Department of Molecular Virology, Immunology, and Medical Genetics; [2]Division of Hematology/Oncology, Department of Internal Medicine; and [3]Center for Biostatistics; Ohio State University, Columbus; and [4]Ohio State University Comprehensive Cancer Center, James Cancer Hospital, and Solove Research Institute, Columbus

Human CD56^{bright} natural killer (NK) cells possess little or no killer immunoglobulin-like receptors (KIRs), high interferon-γ (IFN-γ) production, but little cytotoxicity. CD56^{dim} NK cells have high KIR expression, produce little IFN-γ, yet display high cytotoxicity. We hypothesized that, if human NK maturation progresses from a CD56^{bright} to a CD56^{dim} phenotype, an intermediary NK cell must exist, which demonstrates more functional overlap than these 2 subsets, and we used CD94 expression to test our hypothesis. CD94^{high}CD56^{dim} NK cells express CD62L, CD2, and KIR at levels between CD56^{bright} and CD94^{low}CD56^{dim} NK cells. CD94^{high} CD56^{dim} NK cells produce less monokine-induced IFN-γ than CD56^{bright} NK cells but much more than CD94^{low}CD56^{dim} NK cells because of differential interleukin-12–mediated STAT4 phosphorylation. CD94^{high} CD56^{dim} NK cells possess a higher level of granzyme B and perforin expression and CD94-mediated redirected killing than CD56^{bright} NK cells but lower than CD94^{low}CD56^{dim} NK cells. Collectively, our data suggest that the density of CD94 surface expression on CD56^{dim} NK cells identifies a functional and likely developmental intermediary between CD56^{bright} and CD94^{low}CD56^{dim} NK cells. This supports the notion that, in vivo, human CD56^{bright} NK cells progress through a continuum of differentiation that ends with a CD94^{low}CD56^{dim} phenotype. (Blood. 2010; 115:274-281)

Introduction

Natural killer (NK) cells are CD56^{+}CD3^{-} large granular lymphocytes that constitute approximately 10% of the peripheral blood lymphocytes and represent one component of the innate immune system. NK cells have been recognized as a part of the body's essential first line of defense and play a critical role in combating both infectious pathogens and malignant transformation.[1] NK cells possess rapid cytotoxic capacity and rapid deployment of a variety of cytokines (eg, interferon-γ [IFN-γ] and tumor necrosis factor-α), both of which contribute toward the innate defense.[2-4] Recently, in both murine and human mucosal-associated lymphoid tissue, a novel subset of NK cells, called NK-22 cells, which produces the T_H17 cytokine interleukin-22 (IL-22), and thus probably plays an important role in mucosal immunity, has been identified.[5-11] We recently identified 5 discrete stages of human NK-cell development in secondary lymphoid tissue (SLT)[12,13] and subsequently noted that a majority of stage III immature NK cells constitutively express IL-22, whereas stage IV NK cells are CD56^{bright}, express abundant CD94, and secrete IFN-γ after activation.[8,13]

Mature human NK-cell subsets can be distinguished phenotypically by their relative density of CD56 surface expression. Peripheral blood NK cells are composed of CD56^{bright} (~ 10%) and CD56^{dim} (~ 90%) NK-cell subsets, which are functionally distinct. On activation, CD56^{bright} NK cells proliferate and secrete abundant cytokines, such as IFN-γ, but display minimal cytotoxic activity at rest; in contrast, CD56^{dim} NK cells have little proliferative capacity, produce negligible amounts of monokine-induced IFN-γ, yet are highly cytotoxic at rest.[14,15] Whether these 2 NK-cell subsets represent distinct and terminally differentiated cell types or represent a continuum of NK-cell differentiation has long been debated. There is now some good experimental evidence that NK-cell development proceeds from a CD56^{bright} to CD56^{dim} phenotype,[16-18] yet definitive in vivo proof of this in humans has been elusive. Logic would dictate that, if there is a continuum of NK-cell differentiation from a CD56^{bright} to CD56^{dim} phenotype in vivo, one should be able to identify a subset of "intermediary" NK cells in humans that possess some overlap of the relatively distinct properties attributed to CD56^{bright} and CD56^{dim} cells; however, such a subset has not yet been identified.

CD94 is a type II integral membrane protein that is related to the C-type lectin superfamily[19] and can covalently associate with 5 different members of the NKG2 family (NKG2A, B, C, E, and H), but not with NKG2D.[20] The natural ligand for these CD94/NKG2 heterodimers is the nonclassic major histocompatibility complex class I molecule HLA-E in humans.[20] As noted earlier, human NK cells acquire high surface expression of both CD94 and CD56 at stage IV during NK development in SLT, and this CD94^{high}CD56^{bright} phenotype is coincident with the cell's ability to first secrete abundant IFN-γ after cytokine stimulation.[13]

In the current study, we search for a functional and possible developmental intermediary between the CD56^{bright} NK cell and the CD56^{dim} NK cell using the density of CD94 surface expression. We show that the CD94^{high}CD56^{dim} NK-cell subset has lower granzyme B expression, lower perforin expression, and lower

Submitted April 7, 2009; accepted October 9, 2009. Prepublished online as *Blood* First Edition paper, November 6, 2009; DOI 10.1182/blood-2009-04-215491.

The online version of this article contains a data supplement.

The publication costs of this article were defrayed in part by page charge payment. Therefore, and solely to indicate this fact, this article is hereby marked "advertisement" in accordance with 18 USC section 1734.

CD94-mediated redirected killing compared with the CD94^{low}CD56^{dim} NK-cell subset, although it can traffic to SLT and secrete IFN-γ in response to monokine stimulation with somewhat less potency compared with the CD56^{bright} NK population. The discovery of this functional NK-cell intermediary in vivo supports the notion that the human CD56^{bright} NK cell probably does progress through a continuum of differentiation to become a cytolytic CD94^{low}CD56^{dim} NK cell.

Methods

Reagents

The following fluorescently labeled anti–human monoclonal antibodies (mAbs) were purchased from BD Biosciences PharMingen: CD3, CD25, CD122, CD2, CD43, CD16, CD161, CD117, CD158a (detects KIR2DL1/S1), CD158b (detects KIR2DL2/L3), NKAT2 (detects KIR2DL3), CD62L, CD27, CD11b, HLA-DR, CD69, IFN-γ, and the unconjugated mouse anti–human CD94 mAb (clone HP-3D9). The anti–human antibodies for CD56, NKp30, NKp44, NKp46, NKG2D, NKG2A, and CD158e1/e2 (KIR p70, detects KIR3DL1/S1) were purchased from Beckman Coulter. CCR7, NKG2C, KIR3DL1, and the anti–human CD94 mAb used for cell sorting were purchased from R&D Systems, whereas the CD94 mAb and its isotype control IgG used for phenotypic analysis by flow cytometry were purchased from BD Biosciences PharMingen.

Flow cytometry

NK cells were enriched from peripheral blood leukopacks of healthy donors (American Red Cross, Columbus, OH) using RosetteSep cocktail (StemCell Technologies) as previously described.[21] The enriched NK cells were stained with antibodies and analyzed on a FACSCalibur (BD Biosciences) to detect expression of the indicated antigen. Human NK cells were gated as CD56$^+$CD3$^-$ lymphocytes for further analysis.

Where indicated, 3 NK-cell subsets, CD94^{high}CD56^{bright} (or CD56^{bright}), CD94^{high}CD56^{dim}, or CD94^{low}CD56^{dim}, were sorted by fluorescence-activated cell sorter (FACS) from fresh leukopacks to greater than 98% purity from RosetteSep-cocktail–enriched NK cells after surface staining with CD3, CD56, and CD94 antibodies and gating on CD3$^-$ cells. A typical pre- and post-FACS analysis of the 3 NK-cell subsets is shown in supplemental Figure 1 (available on the *Blood* website; see the Supplemental Materials link at the top of the online article). All experiments were performed with the approval of the Ohio State University Institutional Review Board.

NK-cell stimulation in vitro and IFN-γ detection by enzyme-linked immunosorbent assay and flow cytometry

The aforementioned 3 NK-cell subsets were rested in vitro in 96-well round-bottom plates in medium without cytokines for approximately 2 hours, and an equal number of cells from each subset were then costimulated overnight with recombinant human IL-12 (rhIL-12; 10 ng/mL) plus rhIL-15 (100 ng/mL), or rhIL-12 plus rhIL-18 (100 ng/mL) for indicated time. Supernatants were collected for detection of IFN-γ by enzyme-linked immunosorbent assay (ELISA) as previously described.[21] rhIL-12 was kindly provided by Genetics Institute Inc, rhIL-15 was kindly provided by Amgen, and rhIL-18 was purchased from R&D Systems.

Flow analysis was used to evaluate intracellular IFN-γ content. For this purpose, GolgiPlug (1 μL GolgiPlug per milliliter medium, BD Biosciences PharMingen) was added 4 hours before harvesting cells. The harvested cells were surface stained with anti–CD56-PE, anti–CD3-PEcy7, and anti–CD94-FITC mAbs (BD Biosciences PharMingen), then fixed and permeabilized using Cytofix/Cytoperm (BD Biosciences), and underwent intracellular staining with an anti–human IFN-γ APC mAb (1:25 dilution) or isotype control-APC mAb (BD Biosciences PharMingen). Analyses to estimate IFN-γ production were performed on a FACSCalibur or FACS LSR II cytometer (BD Biosciences) using the CellQuest or Diva (BD Biosciences) software program.

Standard ^{51}Cr release cytotoxicity assay and CD94-mediated redirected killing assay

Cytotoxic activity of each FACS-sorted human NK subset (CD94^{high}CD56^{bright}, CD94^{high}CD56^{dim}, and CD94^{low}CD56^{dim}) against the K562 target cell line was assessed using a standard ^{51}Cr release assay. All sorted NK-cell subsets were added to 5000 ^{51}Cr-labeled K562 target cells per well in triplicate at an effector/target ratio of 2.5:1 or 5.0:1 in 96-well V-bottom plates, which were briefly centrifuged before a 4-hour incubation. After the incubation, supernatants were harvested and counted in a gamma counter to assess ^{51}Cr release as a measure of target cell lysis.

For CD94-mediated redirected killing assay, the sorted 3 NK-cell subsets (CD94^{high}CD56^{bright}, CD94^{high}CD56^{dim}, and CD94^{low}CD56^{dim}) were cultured with IL-2 (100 U/mL) for 4 days. A total of 50 000 cells of each cultured subset were then added to V-bottom wells containing 5000 murine P815 mastocytoma cells (10:1 effector/target), which had been preincubated with the unconjugated anti–human CD94 mouse mAb for 30 minutes, followed by the 4-hour ^{51}Cr release assay.

Real-time polymerase chain reaction

Total mRNA was extracted immediately from the sorted 3 NK-cell subsets (CD94^{high}CD56^{bright}, CD94^{high}CD56^{dim}, and CD94^{low}CD56^{dim}) using a RNeasy kit (QIAGEN) and used to synthesize cDNA according to the manufacturer's instructions (Invitrogen). The primer and probe sequences for human granzyme B (*GZMB*) are as follows: forward primer 5′-TCCTAAGAACTTCTCCAACGACATC-3′, reverse primer 5′-GCACAGCTCTGGTCCGCT-3′, and probe 5′-FAM-TGCTACTG-CAGCTGGAGAGAAAGGCC-3′TAMRA; for perforin 1 (*PRF1*) are as follows: forward primer 5′-CAGCACTGACACGGTGGAGT-3′, reverse primer 5′GTCAGGGTGCAGCGGG-3′, and probe 5′FAM-CCGCTTCTACAGTTTCCATGTGGTACACACTC-3′TAMRA. Real-time polymerase chain reaction (PCR) was performed on an ABI Prism 7900HT (Applied Biosystems), normalized to an 18S internal control and then analyzed by the ΔΔCt method as previously described.[21]

Western blotting

To assess STAT signaling, direct cell lysates or total protein extractions were prepared from sorted CD94^{high}CD56^{dim} and CD94^{low}CD56^{dim} NK-cell subsets treated for 30 minutes in media with or without rhIL-12 (10 ng/mL), rhIL-12 plus rhIL-15 (100 ng/mL), or rhIL-12 plus rhIL-18 (100 ng/mL). Western blotting was performed as previously described.[21] Assessment of β-actin by Western blotting was included to control for protein loading. Antibodies used for Western blotting are as follows: rabbit mAb phospho-STAT5^{Tyr694} (Cell Signaling), rabbit mAb phospho-STAT4^{Tyr693} (Invitrogen), rabbit mAb phospho-STAT3^{Tyr705} (Cell Signaling), mouse mAb STAT4 (Invitrogen), and goat polyclonal Ab β-actin (Santa Cruz Biotechnology).

Statistical analysis

Because repeated measures were collected from the same donors for many outcomes, linear mixed effects models or paired *t* test was used for analysis by taking into account the dependency of these repeated measures. The Tukey method was used to correct for multiple comparisons, and the adjusted *P* value was calculated. An adjusted *P* value less than .05 is considered significant for a comparison test among multiple comparisons.

Results

Phenotypic dissection of CD56^{dim} NK-cell subsets based on the relative density of CD94 surface expression

We first gated on CD3$^-$CD56$^+$ NK cells for assessment of CD94 expression. It was noted that nearly all CD56^{bright} NK cells, which are thought to be the most potent NK-cell subset for IFN-γ

production in humans, are CD94^{high}. However, the density of CD94 surface expression on the CD56^{dim} NK-cell population segregated CD94^{high} and CD94^{low} subsets (Figure 1A). Accordingly, we refer to 3 human NK-cell subsets in the current study: CD94^{high}CD56^{bright}, CD94^{high}CD56^{dim}, and CD94^{low}CD56^{dim}, which in blood from 14 normal donors accounted for approximately 8%, 53%, and 39% of NK cells, respectively (Figure 1A). The density of CD94 surface expression in CD94^{low} and CD94^{high} human NK-cell subsets was confirmed by staining identically processed cells from the same donor with an isotype control antibody and gating on the same population, as shown in Figure 1B.

Surface expression of NK receptors often corresponds to NK maturation and function.[12,13,22] We therefore examined the expression patterns of several receptors in the aforementioned NK-cell subsets by flow-cytometric analysis (Figure 2). Compared with both the CD94^{high}CD56^{dim} and the CD94^{low}CD56^{dim} NK-cell subsets, proportionally the CD94^{high}CD56^{bright} subset has higher expression of CD117 ($P < .003$ for each comparison), CD62L ($P < .001$), and CD27 ($P < .001$), as well as lower expression of CD16 ($P < .001$) and killer immunoglobulin-like receptors (KIRs; KIR2DL1/S1, KIR2DL2/L3, KIR3DL1/S1, KIR2DL3, and KIR3DL1; $P < .05$ for each), which are consistent with previous studies showing differential expression of these surface markers between CD56^{bright} and CD56^{dim} NK cells.[23,24] In addition, however, we found that a greater fraction of the CD94^{high}CD56^{bright} NK-cell subset expresses NKp44 and CCR7 compared with either of the 2 CD56^{dim} subsets ($P < .001$ for each comparison), which were similar to each other in expression for these 2 molecules. Interestingly, NKG2A appears to be expressed exclusively on the 2 CD94^{high} subsets (CD94^{high}CD56^{bright} and CD94^{high}CD56^{dim}) but absent on the CD94^{low} subset (CD94^{low}CD56^{dim}). The CD94^{high}CD56^{bright} and CD94^{high}CD56^{dim} subsets appear to have a minor yet discernable

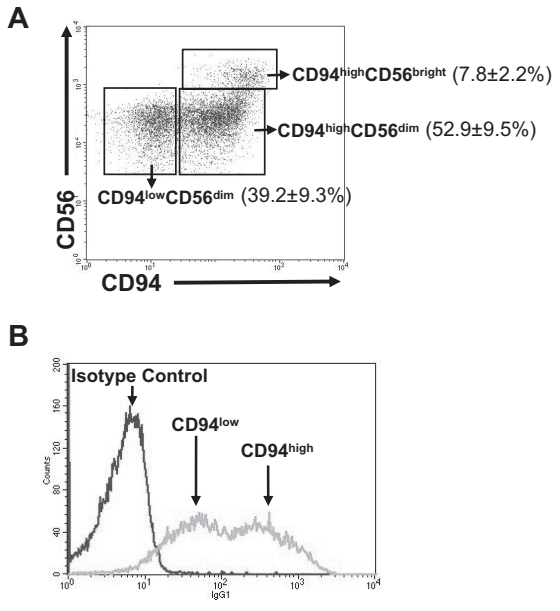

Figure 1. Dissection of human CD56$^+$CD3$^-$ NK-cell subsets by CD94 surface expression. (A) Mononuclear cells freshly isolated from peripheral blood were stained with anti-CD3, anti-CD56, and anti-CD94 fluorescently labeled mAb. CD56$^+$CD3$^-$ NK cells were then gated for quantification of CD94 surface density. The dot plot shown is for a representative donor, and the numbers in the plot are averaged from 14 healthy donors and represent the percentage of total NK cells ± SD belonging to each subset of CD94^{high}CD56^{bright}, CD94^{high}CD56^{dim} and CD94^{low}CD56^{dim}. (B) Comparison of CD94-PE antibody staining (gray) and its isotype control IgG1-PE staining (black) of NK cells gated on CD56$^+$CD3$^-$.

association with NKG2C expression, whereas the CD94^{low} CD56^{dim} subset does not. Finally, we noted that the density of surface expression of CD62L, CD2, and all tested KIRs on the CD94^{high}CD56^{dim} NK-cell subset is at an "intermediate" level between that seen on the CD94^{high}CD56^{bright} NK-cell subset and on the CD94^{low}CD56^{dim} NK-cell subset (Figure 2).

The capacity of the monokine-activated CD94^{high}CD56^{dim} NK subset to produce IFN-γ is intermediate to that of the CD94^{high}CD56^{bright} and CD94^{low}CD56^{dim} NK-cell subsets

To compare IFN-γ production from the monokine-activated CD94^{high}CD56^{bright}, CD94^{high}CD56^{dim}, and CD94^{low}CD56^{dim} NK-cell subsets circulating in blood, enriched NK cells were costimulated in vitro with IL-12 and IL-18. Intracellular flow analysis was then used to measure IFN-γ production within each of these subsets, as assessed by the percentage of the IFN-γ$^+$ cells. Consistent with our previous study,[14] we found that the fraction of IFN-γ$^+$ cells was greatest in the CD94^{high}CD56^{bright} subset. Notably, when gating on CD56^{dim} NK cells, the CD94^{high}CD56^{dim} subset responded to costimulation by IL-12 and IL-18 with fairly robust IFN-γ production, whereas the CD94^{low}CD56^{dim} subset had negligible IFN-γ production, virtually lacking any IFN-γ$^+$ cells (Figure 3A left panel; supplemental Figure 2). We also noticed that more than half of the CD94^{high}CD56^{dim} cells do not produce any INF-γ, which is much like the entire CD94^{low}CD56^{dim} NK-cell subset (Figure 3A left, Figure 3B). This is in contrast to the CD94^{high}CD56^{bright} NK-cell subset where virtually 100% of the cells respond to this costimulus with production of IFN-γ (Figure 3B). ELISA results measuring IFN-γ secretion from an equal number of the 3 NK-cell subsets stimulated by IL-12 and IL-18 (Figure 3A right panel) confirmed the data obtained using intracellular flow cytometry. In addition to demonstrating this gradation of IFN-γ production among these NK subsets, the data also identify an NK-cell subset in fresh blood that is virtually void of any IFN-γ production, even on costimulation by IL-12 and IL-18, which has been previously described as the strongest monokine stimulus for NK cell IFN-γ production. Similar results were obtained using ELISA and real-time PCR to analyze IFN-γ expression of the subsets costimulated with IL-12 and IL-15 when equal numbers of the cells from each of subset were used (Figure 3C). To compare capacity of CD94^{high}CD56^{dim} and CD94^{low}CD56^{dim} NK-cell subsets for IFN-γ production in the context of tumor-host interactions, freshly enriched NK cells were cocultured with K562 tumor cells for 48 hours in the absence of cytokines. Supplemental Figure 3 shows intracellular flow for IFN-γ indicating that CD94^{high}CD56^{dim} NK cells produce significantly more IFN-γ than CD94^{low}CD56^{dim} NK cells after their interaction with tumor cells.

Assessment of cytotoxic activity in CD94^{high}CD56^{bright}, CD94^{high}CD56^{dim}, and CD94^{low}CD56^{dim} subsets

We assessed granzyme B and perforin 1 gene expression among the 3 subsets. The CD94^{high}CD56^{bright}, CD94^{high}CD56^{dim}, and CD94^{low}CD56^{dim} subsets showed a low, intermediate, and high level of expression for both genes, respectively (Figure 4A-B). Consistent with this, CD94-mediated redirected killing among the 3 NK-cell subsets correlated with the expression level granzyme B and perforin 1, in that the CD94^{high}CD56^{dim} NK cells show an intermediate level of cytotoxic activity compared

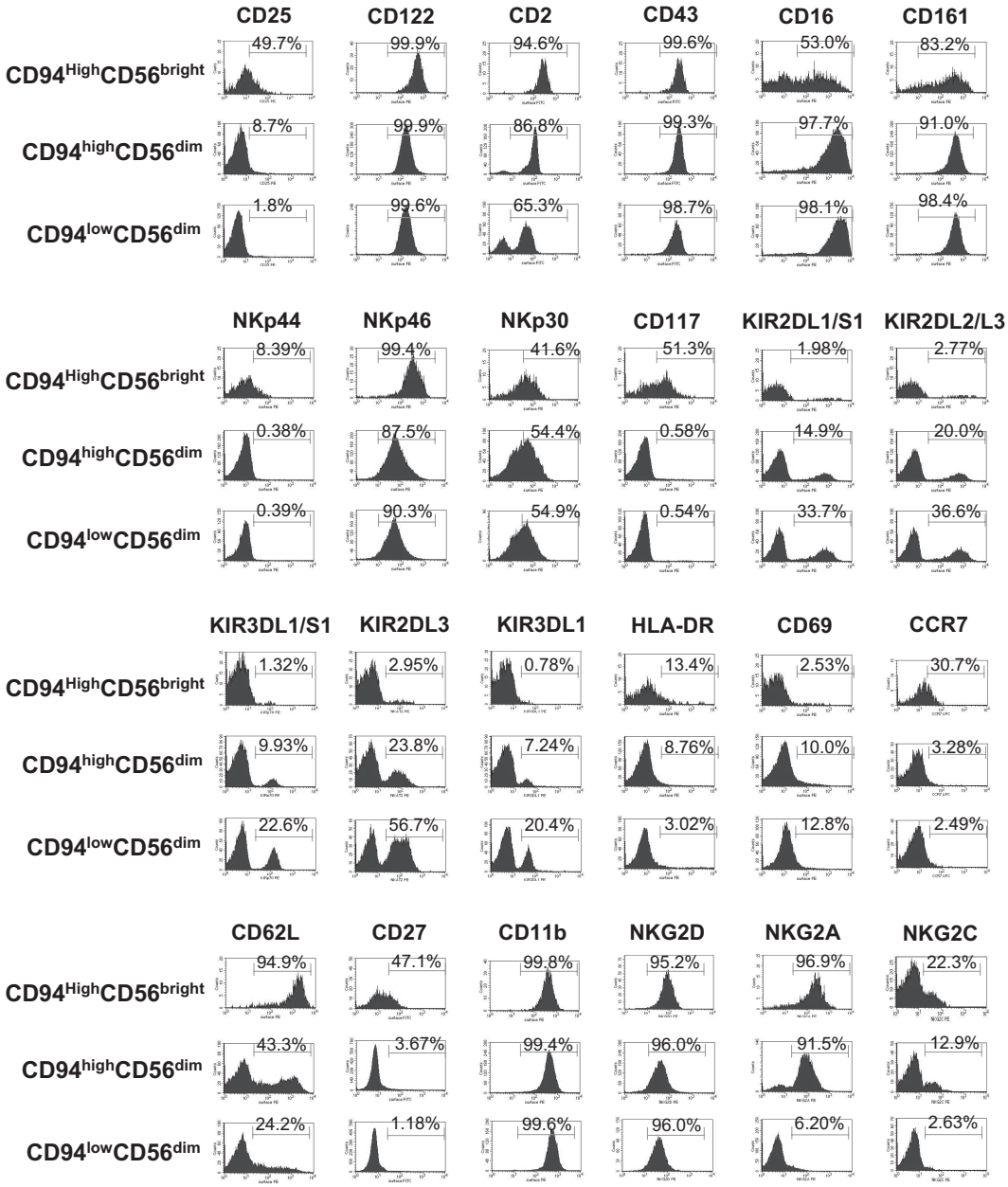

Figure 2. Quantification of surface antigen expression on human NK subsets defined by CD56 and CD94. Peripheral blood NK cells were enriched to purity 50% to 85% using RosetteSep cocktail and then stained with anti-CD3, anti-CD56, and anti-CD94–conjugated mAb, as well as a mAb directed against the surface antigens indicated in each histogram. Each of the 3 gated populations (CD94^{high}CD56^{bright}, CD94^{high}CD56^{dim}, and CD94^{low}CD56^{dim}) was then assessed for positivity for surface expression of the fourth antigen as shown compared with its isotype control (not shown). The number in each histogram shows the percentage of cells that are positive for the indicated antigen(s), and is averaged from at least 3 different normal donors.

with the CD94^{high}CD56^{bright} and the CD94^{low}CD56^{dim} subsets (Figure 4C).

When we assessed natural cytotoxicity of fresh NK cells against the K562 tumor cell line by a standard ^{51}Cr release assay, we found that the CD94^{high}CD56^{bright} cell subset has much lower cytotoxicity than CD94^{high}CD56^{dim} and CD94^{low}CD56^{dim} NK subsets, consistent with a previous report comparing CD56^{bright} and CD56^{dim}.[15] However, we found no consistent difference in cytotoxic activity between the CD94^{high}CD56^{dim} and CD94^{low}CD56^{dim} NK subsets. (Table 1 summarizes data from 8 donors.) Likewise, we noted that CD107a expression between these 2 CD56^{dim} NK subsets is not statistically significant when undergoing natural cytotoxicity against K562 target cells (not shown). This similarity in natural cytotoxicity could in part be related to the nearly equivalent amounts of major triggering receptors (eg, NKp30) expressed on the surface of these 2 CD56^{dim} subsets as noted in Figure 2, despite significantly lower amounts of intracellular perforin and granzyme B in the CD94^{high}CD56^{dim} population.

In the presence of IL-12, the CD94^{high}CD56^{dim} NK-cell subset has greater STAT4 phosphorylation than the CD94^{low}CD56^{dim} NK-cell subset

Next, we pursued the molecular mechanisms by which the CD94^{high}CD56^{dim} NK-cell subset has significantly more IFN-γ production compared with the CD94^{low}CD56^{dim} NK-cell subset. We first purified CD94^{high}CD56^{dim} and CD94^{low}CD56^{dim} NK-cell subsets by FACS, and compared relevant transcript levels within these 2 NK-cell subsets. We found that, in both resting and

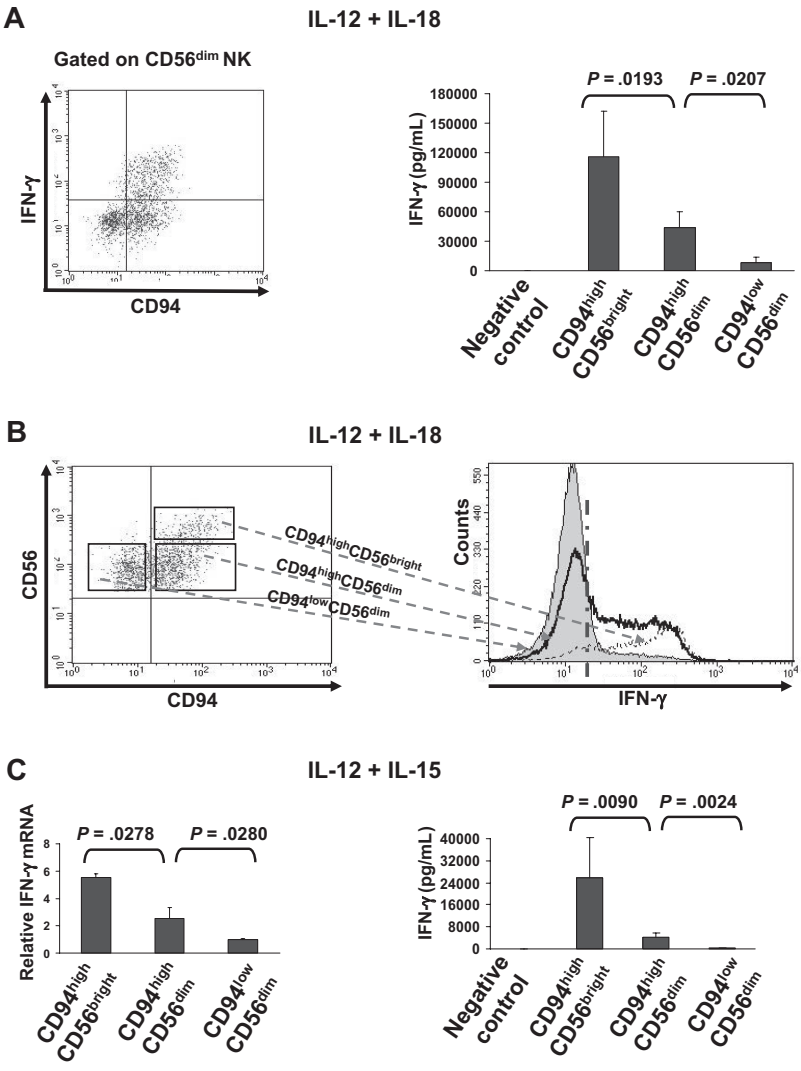

Figure 3. CD94 identifies functionally distinct human CD56^{dim} NK-cell subsets with regard to IFN-γ production. (A left panel) Enriched NK cells were costimulated with IL-12 and IL-18 for 24 hours followed by intracellular staining for IFN-γ. After gating on CD56^{dim}CD3^{-} cells, density of CD94 surface expression and intracellular IFN-γ production were simultaneously assessed as shown in the representative dot plot. (A right panel) Equal numbers of the 3 NK-cell subsets were stimulated with IL-12 plus IL-18, followed by measurement of secreted IFN-γ using ELISA. (B) Relative comparison of each of the 3 NK-cell subsets (left) costimulated by IL-12 and IL-18 for 24 hours in ability to produce IFN-γ using intracellular flow-cytometric analysis (right). Cells on the right side of the dashed vertical line are positive for IFN-γ. The figures are representative of at least 3 separate experiments. (C) Equal numbers of the 3 NK-cell subsets were stimulated with IL-12 plus IL-15 for 24 hours, followed by measurement of IFN-γ mRNA by real-time PCR (left) as well as secreted IFN-γ by ELISA (right). Bar graphs (A,C) represent mean ± SD for at least 3 experiments. Enriched NK cells under no monokine stimulation were used as a negative control for IFN-γ ELISA assay (A,C).

activated CD56^{dim} NK cells, the CD94^{high}CD56^{dim} NK-cell subset has significantly lower mRNA expression of several KIRs (eg, KIR2DL1, KIR2DL3, KIR2DL4, KIR2DS1, KIR2DS3, KIR2DS4, KIR2DL5A, KIR3DL2, KIR3DL3, and KIR3DS1) compared with the CD94^{low}CD56^{dim} NK-cell subset ($P < .05$ for each, data not shown), consistent with the level of surface expression determined by flow cytometry (Figure 2). Our analysis could not detect significant differences in IL-12R, IL-15R, or IL-18R mRNA expression between the CD94^{high}CD56^{dim} and CD94^{low}CD56^{dim} NK-cell subsets. Real-time reverse-transcription-PCR indicated that there is also no difference between the CD94^{high}CD56^{dim} and CD94^{low}CD56^{dim} NK-cell subset expression of *T-BET*, which regulates IFN-γ production (data not shown).

We continued to assess known downstream signaling mediators of IL-12, IL-15, and IL-18 receptors. Although their downstream STAT signaling mediators have been previously shown to play critical roles in positively regulating NK-cell function, especially regarding IFN-γ production,[25] real-time reverse-transcription-PCR and/or Western blotting demonstrated that there were no differences between the CD94^{high} CD56^{dim} and CD94^{low}CD56^{dim} NK-cell subsets in their expression of total STAT3, STAT4, and STAT5 (Figure 5A-B; and data not shown). We therefore continued by analyzing the activation state of these STAT proteins. There was no difference in STAT3 and STAT5 phosphorylation between the CD94^{high}CD56^{dim} and CD94^{low}CD56^{dim} NK-cell subsets costimulated by IL-12 and IL-15 for 30 minutes. There was also no significant difference in the STAT4 phosphorylation level between CD94^{high}CD56^{dim} and CD94^{low}CD56^{dim} NK-cell subsets in the absence of cytokine stimulation (Figure 5B). However, Western blotting showed that the CD94^{high}CD56^{dim} NK-cell subset possessed higher STAT4 phosphorylation than the CD94^{low}CD56^{dim} NK-cell subset after stimulation by IL-12 alone, IL-12 plus IL-15, or IL-12 plus IL-18 (Figure 5B-C). Collectively, the molecular data shown here suggest that the enhanced IFN-γ production seen within the monokine-stimulated CD94^{high}CD56^{dim} NK-cell subset can be explained, at least in part, by its selectively greater phosphorylation of STAT4 in the presence of IL-12.

Discussion

Previously, we and others found that human NK cells could be separated into 2 functionally distinct subsets based on the surface density of CD56 (ie, CD56^{bright} and CD56^{dim}). CD56^{bright} NK cells are highly proliferative and produce abundant cytokines in response to monokine costimulation with little natural cytotoxicity at

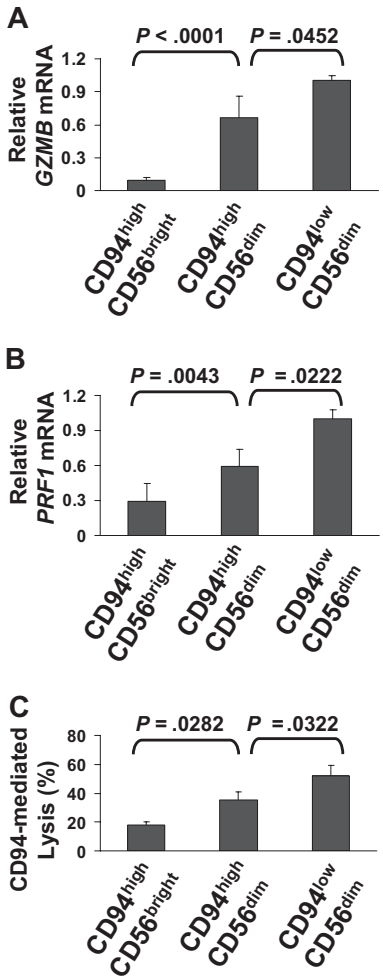

Figure 4. The CD94^{high}CD56^{dim} NK-cell subset shows an intermediate level of granzyme B and perforin 1 gene expression and CD94-mediated redirected killing compared with the CD94^{high}CD56^{bright} and the CD94^{low}CD56^{dim} NK-cell subsets. (A-B) Real-time PCR analysis of *GZMB* (A) and *PRF1* (B) using cDNA from the freshly sorted CD94^{high}CD56^{bright}, CD94^{high}CD56^{dim}, and CD94^{low}CD56^{dim} NK-cell subsets. Data are summarized from 6 donors, and the error bars represent SD. (C) ^{51}Cr cytotoxicity analysis of the aforementioned sorted 3 NK-cell subsets against the murine cell line P815 in the presence of the purified anti–human CD94 mouse mAb. Data are summarized from 3 donors, and the error bars represent SD.

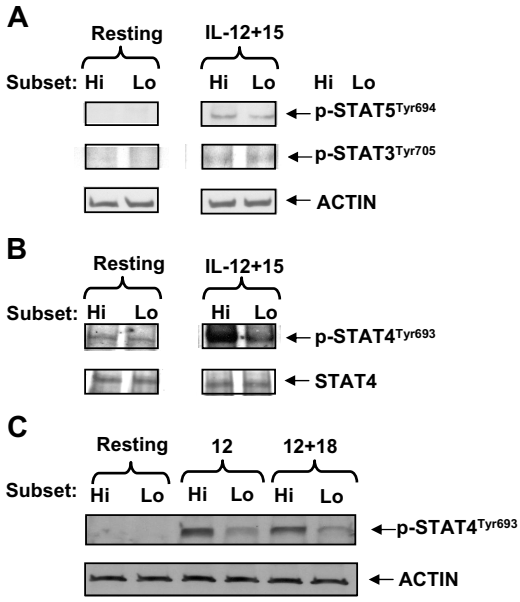

Figure 5. The CD94^{high}CD56^{dim} NK-cell subset possesses higher STAT4 phosphorylation than the CD94^{low}CD56^{dim} NK-cell subset. (A-B) Purified CD94^{high} CD56^{dim} (Hi) and CD94^{low}CD56^{dim} (Lo) NK-cell subsets were cultured in media in the presence or absence of costimulation with rhIL-12 (10 ng/mL) and rhIL-15 (100 ng/mL) for 30 minutes. Lysates from these cells were used to determine the level of STAT5, and STAT3 (A) or STAT4 (B) phosphorylation by Western blotting. Assessment of β-actin or total STAT4 was included to control for protein loading. (C) CD94^{high}CD56^{dim} (Hi) and CD94^{low}CD56^{dim} (Lo) NK-cell subsets were treated in media with or without rhIL-12 alone or costimulation by IL-12 and IL-18 for 30 minutes. Lysates from the harvested cells were used to detect STAT4 phosphorylation. β-Actin was included to control for protein loading. Data in panels A to C are representative of at least 3 experiments with similar results.

rest, whereas CD56^{dim} NK cells proliferate poorly and are inefficient at cytokine production, yet have potent natural and antibody-dependent cytotoxic activity.[14,15] There has been controversy as to whether these 2 NK-cell subsets are each terminally differentiated or whether the CD56^{bright} NK cell ultimately differentiates into the CD56^{dim} NK cell. In the current study, we hypothesized that, if there is a continuum of differentiation along the NK-cell lineage from CD56^{bright} to CD56^{dim}, then a functional intermediary found in vivo between these 2 NK cells should be realized. Indeed, here we report that surface density of CD94, a receptor that first appears at stage IV during NK-cell development in SLT,[13] could be used to further dissect the CD56^{dim} NK-cell subset into CD94^{high}CD56^{dim} and CD94^{low}CD56^{dim} NK-cell subsets.

Supporting a model in which developmental progression occurs from CD94^{high}CD56^{bright} NK cell to CD94^{high}CD56^{dim} NK cell and finally to the CD94^{low}CD56^{dim} NK cell, we found a successive and significant decrease in cytokine-mediated proliferation (not shown) and IFN-γ production, an increase in granzyme B and perforin 1 expression, and CD94-mediated redirected killing, whereas the

Table 1. Variability of natural cytotoxicity of CD94^{high}CD56^{bright}, CD94^{high}CD56^{dim}, and CD94^{low}CD56^{dim} NK-cell subsets

	Effector/target 5:1			Effector/target 2.5:1		
Donor	CD94^{high}CD56^{bright}	CD94^{high}CD56^{dim}	CD94^{low}CD56^{dim}	CD94^{high}CD56^{bright}	CD94^{high}CD56^{dim}	CD94^{low}CD56^{dim}
1	26.5	53.9	73.9	21.6	21.7	54.0
2	20.4	34.3	52.4	12.2	22.6	39.2
3	35.5	63.8	57.1	17.8	66.3	42.8
4	28.9	44.8	71.2	19.5	20.5	42.6
5	54.8	72.9	67.7	34.9	54.5	63.1
6	25.6	62.7	63.4	16.9	53.2	44.1
7	ND	42.2	32.6	9.7	36.5	17.0
8	19.3	49.8	45.7	13.3	38.5	29.9
Mean	30.1 ± 12.1	53.1 ± 12.8	58.0 ± 14.0	18.2 ± 7.7	39.2 ± 17.3	41.6 ± 14.0
*P**		.498			.909	

Data are percentage of natural cytotoxicity against the K562 cell line.
**P* value between CD94^{high}CD56^{dim} and CD94^{low}CD56^{dim} NK-cell subsets.

latter 2 subsets showed no significant difference in natural cytotoxic activity at rest. The significant difference in cytokine-mediated IFN-γ production noted between the CD94^{high}CD56^{dim} and CD94^{low}CD56^{dim} NK-cell subsets could be mechanistically explained by the magnitude of STAT4 phosphorylation in response to IL-12. Hence, by quantifying surface density of CD94 on the CD56^{dim} NK-cell subset, we have been able to identify an NK-cell intermediary that functionally sits between the previously described CD56^{bright} NK cell and the CD56^{dim} NK cell in blood, supporting the notion that, in humans, the CD56^{bright} NK cell does indeed differentiate into a CD56^{dim} NK cell in vivo.

In mice, Smyth et al described the CD27^{high} NK cells as producing more IFN-γ and possessing higher cytotoxicity than CD27^{low} NK cells.[24,26] The van Lier group found that CD27^{+} human NK cells are mainly from the CD56^{bright} subset,[24] which we confirmed in this study, and secrete much more IFN-γ than CD27^{-} NK cells. CD27^{-} NK cells were largely CD56^{dim} and show stronger cytotoxicity than CD27^{+} NK cells. To test whether there is a functional intermediary between CD56^{bright} and CD56^{dim} in humans, we chose to use CD94 surface expression, given our earlier studies pointing to the relevance of CD94 surface expression to human NK-cell development.[13]

NK receptors are tightly linked to NK-cell development and function.[12,13,22] Compared with CD56^{dim} NK cells, CD56^{bright} NK cells have higher surface expression of CD117, the receptor of stem cell factor also found on the hematopoietic precursor cell, as well as CD62L and CD27; the CD56^{bright} NK-cell subset has lower expression of cytotoxicity receptors CD16 and KIR, suggesting that CD56^{bright} NK cells may represent an earlier stage of NK-cell development, if not a terminal stage.[27] Indeed, in an experimental system, CD56^{bright} NK cells have been reported to differentiate into CD56^{dim} NK cells through contact with peripheral fibroblasts.[16] Interestingly, when CD94^{high}CD56^{bright}, CD94^{high}CD56^{dim}, and CD94^{low}CD56^{dim} NK-cell subsets were compared with each other in our study, the CD94^{high}CD56^{dim} subset expressed an intermediate level of some surface markers, consistent with our notion of a differentiation pathway whereby CD94^{high}CD56^{bright} NK cells develop into CD94^{high}CD56^{dim} first and then terminally differentiate into CD94^{low}CD56^{dim} NK cells. In agreement with this, we demonstrate that the expression level of "immature" NK cell marker CD62L on CD94^{high}CD56^{dim} NK cells is lower than is seen on CD94^{high}CD56^{bright} NK cells but higher than that seen on CD94^{low}CD56^{dim} NK cells. Likewise, as demonstrated in this study, CD94^{high}CD56^{dim} NK cells are "bifunctional" in that they retain some ability to produce IFN-γ (albeit it less than the CD94^{high} CD56^{bright} NK-cell subset on a per-cell basis) yet still have an intermediate level of CD94-mediated redirected killing and a high level of natural cytotoxicity compared with the CD94^{low}CD56^{dim} NK cells that have virtually no ability to proliferate (not shown) or secrete IFN-γ. The fact that only approximately half of the CD94^{high}CD56^{dim} NK cells can produce IFN-γ in response to IL-12 and IL-18 (compared with the CD94^{high}CD56^{bright} NK cells which all produce IFN-γ) is again in keeping with this notion of a continuum along a pathway of NK-cell differentiation. The same analogy that has been made for IFN-γ secretion among these 3 subsets can be made for NK-cell proliferation (not shown).

The significantly higher surface expression of CD62L that is noted on the CD94^{high}CD56^{dim} NK-cell subset compared with the CD94^{low}CD56^{dim} NK-cell subset probably allows the former subset to traffic into SLT via high endothelial venules where it may undergo activation to secrete IFN-γ by interaction with IL-12–secreting dendritic cells. The significantly lower expression of CD62L on CD94^{low}CD56^{dim} NK cells probably limits their ability to traffic into SLT for activation with dendritic cells. Thus, the correlation between intermediate CD62L expression on the CD94^{high}CD56^{dim} NK-cell subset and its intermediate ability to secrete IFN-γ in response to IL-12–secreting dendritic cells is probably more than coincidental. The CD56^{bright} NK cell has the highest CD62L expression, along with high CCR7 expression, and this probably contributes to its predominance in SLT compared with its relatively minor presence in blood.[28, 29]

In attempting to explain the difference in cytokine-mediated IFN-γ secretion seen between the CD94^{high}CD56^{dim} and CD94^{low}CD56^{dim} human NK cells, we excluded differences in monokine receptor gene expression or differences in activated STAT3 or STAT5, both of which mediate IL-15 signaling and the former of which can also mediate IL-18 signaling.[30-32] We discovered that STAT4 phosphorylation, induced by the potent IFN-γ stimulus IL-12,[33] is significantly greater in the CD94^{high}CD56^{dim} NK-cell subset compared with the CD94^{low}CD56^{dim} NK-cell subset. This difference in STAT4 activation may be the result of varied intracellular levels of a STAT4 kinase or phosphatase, and this will require further study.

Another explanation for our findings could relate to CD62L expression, which parallels CD94 expression in that it is highest on CD94^{high}CD56^{bright} NK cells and moderately high on CD94^{high} CD56^{dim} NK cells yet is significantly lower on CD94^{low}CD56^{dim} NK cells. Activation signals within SLT, possibly induced or amplified by NK-cell IFN-γ secretion, may contribute to continued CD62L expression and NK retention within or migration to SLT. As activation within SLT subsides, CD62L expression would diminish and retention within or migration to SLT would cease. Indeed, in the absence of continued stimulation from monokines found within activated SLT, transcription factors that induce NK cytokine production such as *TBET* may diminish.[21] In this model, the gradual decrease in migration in and out of SLT, as dictated by CD62L expression, would contribute to a decrease in cytokine-induced NK-cell activation and continued NK-cell differentiation.

In conclusion, we used CD94 surface density on human NK cells to identify a phenotypic and functional intermediary that exists between the previously defined CD56^{bright} and CD56^{dim} NK-cell subsets. The ex vivo characterization of the CD94^{high} CD56^{dim} and CD94^{low}CD56^{dim} NK-cell subsets lends further support in favor of an in vivo continuum of NK-cell differentiation from the CD56^{bright} NK cell that predominates in SLT to the CD94^{low}CD56^{dim} NK cell that predominates in blood. The signals promoting the process of NK-cell differentiation probably reside within SLT but will require additional study for elucidation.

Acknowledgments

This work was supported by the Flow Cytometry, Biostatistics Center, and Nucleic Acid Shared Resources within the Ohio State University Comprehensive Cancer Center, the National Cancer Institute (grants CA95426 and CA68458; M.A.C.), and the Division of Human Cancer Genetics at Ohio State University (Up on the Roof Fellowship; J.Y.).

Authorship

Contribution: J.Y. codesigned and performed the research work and wrote the manuscript; H.C.M. and M.W. performed research work;

T.H., I.-k.P., S.L., S.M., G.M., and R.T. designed some of the research work; J.Z. analyzed data; and M.A.C. codesigned the research work and wrote the manuscript.

Conflict-of-interest disclosure: The authors declare no competing financial interests.

Correspondence: Michael A. Caligiuri, Ohio State University, 300 W 10th Ave, Suite 521C, Columbus, OH 43210; e-mail: michael.caligiuri@osumc.edu; and Jianhua Yu, Ohio State University, 460 W 12th Ave, Rm 882, Columbus, OH 43210; e-mail: jianhua.yu@osumc.edu.

References

1. Liu CC, Perussia B, Cohn ZA, Young JD. Identification and characterization of a pore-forming protein of human peripheral blood natural killer cells. *J Exp Med.* 1986;164(6):2061-2076.
2. Kim S, Iizuka K, Aguila HL, Weissman IL, Yokoyama WM. In vivo natural killer cell activities revealed by natural killer cell-deficient mice. *Proc Natl Acad Sci U S A.* 2000;97(6):2731-2736.
3. Smyth MJ, Hayakawa Y, Takeda K, Yagita H. New aspects of natural-killer-cell surveillance and therapy of cancer. *Nat Rev Cancer.* 2002;2(11): 850-861.
4. Dorner BG, Smith HR, French AR, et al. Coordinate expression of cytokines and chemokines by NK cells during murine cytomegalovirus infection. *J Immunol.* 2004;172(5):3119-3131.
5. Luci C, Reynders A, Ivanov II, et al. Influence of the transcription factor RORgammat on the development of NKp46+ cell populations in gut and skin. *Nat Immunol.* 2009;10(1):75-82.
6. Cella M, Fuchs A, Vermi W, et al. A human natural killer cell subset provides an innate source of IL-22 for mucosal immunity. *Nature.* 2009; 457(7230):722-725.
7. Zenewicz LA, Yancopoulos GD, Valenzuela DM, Murphy AJ, Stevens S, Flavell RA. Innate and adaptive interleukin-22 protects mice from inflammatory bowel disease. *Immunity.* 2008;29(6):947-957.
8. Hughes T, Becknell B, McClory S, et al. Stage three immature human natural killer cells found in secondary lymphoid tissue constitutively and selectively express the TH17 cytokine interleukin-22. *Blood.* 2009;113(17):4008-4010.
9. Cooper MA, Colonna M, Yokoyama WM. Hidden talents of natural killers: NK cells in innate and adaptive immunity. *EMBO Rep.* 2009;10(10): 1103-1110.
10. Colonna M. Interleukin-22-producing natural killer cells and lymphoid tissue inducer-like cells in mucosal immunity. *Immunity.* 2009;31(1):15-23.
11. Satoh-Takayama N, Vosshenrich CA, Lesjean-Pottier S, et al. Microbial flora drives interleukin 22 production in intestinal NKp46+ cells that provide innate mucosal immune defense. *Immunity.* 2008;29(6):958-970.
12. Freud AG, Caligiuri MA. Human natural killer cell development. *Immunol Rev.* 2006;214:56-72.
13. Freud AG, Yokohama A, Becknell B, et al. Evidence for discrete stages of human natural killer cell differentiation in vivo. *J Exp Med.* 2006; 203(4):1033-1043.
14. Cooper MA, Fehniger TA, Turner SC, et al. Human natural killer cells: a unique innate immunoregulatory role for the CD56(bright) subset. *Blood.* 2001;97(10):3146-3151.
15. Nagler A, Lanier LL, Cwirla S, Phillips JH. Comparative studies of human FcRIII-positive and negative natural killer cells. *J Immunol.* 1989; 143(10):3183-3191.
16. Chan A, Hong DL, Atzberger A, et al. CD56bright human NK cells differentiate into CD56dim cells: role of contact with peripheral fibroblasts. *J Immunol.* 2007;179(1):89-94.
17. Ouyang Q, Baerlocher G, Vulto I, Lansdorp PM. Telomere length in human natural killer cell subsets. *Ann N Y Acad Sci.* 2007;1106:240-252.
18. Romagnani C, Juelke K, Falco M, et al. CD56brightCD16- killer Ig-like receptor-NK cells display longer telomeres and acquire features of CD56dim NK cells upon activation. *J Immunol.* 2007;178(8):4947-4955.
19. Chang C, Rodriguez A, Carretero M, Lopez-Botet M, Phillips JH, Lanier LL. Molecular characterization of human CD94: a type II membrane glycoprotein related to the C-type lectin superfamily. *Eur J Immunol.* 1995;25(9):2433-2437.
20. Borrego F, Masilamani M, Marusina AI, Tang X, Coligan JE. The CD94/NKG2 family of receptors: from molecules and cells to clinical relevance. *Immunol Res.* 2006;35(3):263-278.
21. Yu J, Wei M, Becknell B, et al. Pro- and antiinflammatory cytokine signaling: reciprocal antagonism regulates interferon-gamma production by human natural killer cells. *Immunity.* 2006;24(5): 575-590.
22. Kim S, Iizuka K, Kang HS, et al. In vivo developmental stages in murine natural killer cell maturation. *Nat Immunol.* 2002;3(6):523-528.
23. Cooper MA, Fehniger TA, Caligiuri MA. The biology of human natural killer-cell subsets. *Trends Immunol.* 2001;22(11):633-640.
24. Vossen MT, Matmati M, Hertoghs KM, et al. CD27 defines phenotypically and functionally different human NK-cell subsets. *J Immunol.* 2008;180(6): 3739-3745.
25. Schoenborn JR, Wilson CB. Regulation of interferon-gamma during innate and adaptive immune responses. *Adv Immunol.* 2007;96:41-101.
26. Hayakawa Y, Smyth MJ. CD27 dissects mature NK cells into two subsets with distinct responsiveness and migratory capacity. *J Immunol.* 2006; 176(3):1517-1524.
27. Caligiuri MA. Human natural killer cells. *Blood.* 2008;112(3):461-469.
28. Frey M, Packianathan NB, Fehniger TA, et al. Differential expression and function of L-selectin on CD56bright and CD56dim natural killer cell subsets. *J Immunol.* 1998;161(1):400-408.
29. Fehniger TA, Cooper MA, Nuovo GJ, et al. CD56bright natural killer cells are present in human lymph nodes and are activated by T cell-derived IL-2: a potential new link between adaptive and innate immunity. *Blood.* 2003;101(8): 3052-3057.
30. McInnes IB, Gracie JA. Interleukin-15: a new cytokine target for the treatment of inflammatory diseases. *Curr Opin Pharmacol.* 2004;4(4):392-397.
31. Nakanishi K, Yoshimoto T, Tsutsui H, Okamura H. Interleukin-18 regulates both Th1 and Th2 responses. *Annu Rev Immunol.* 2001;19:423-474.
32. Ohteki T. Critical role for IL-15 in innate immunity. *Curr Mol Med.* 2002;2(4):371-380.
33. Watford WT, Hissong BD, Bream JH, Kanno Y, Muul L, O'Shea JJ. Signaling by IL-12 and IL-23 and the immunoregulatory roles of STAT4. *Immunol Rev.* 2004;202:139-156.